Available online at www.sciencedirect.com
ScienceDirect
Trans. Nonferrous Met. Soc. China 30(2020) 1078−1090
Transactions of Nonferrous Metals Society of China
www.tnmsc.cn

Catalytic effect of visible light and Cd^{2+} on chalcopyrite bioleaching

Chun-xiao ZHAO, Bao-jun YANG, Xing-xing WANG, Hong-bo ZHAO, Min GAN, Guan-zhou QIU, Jun WANG

Key Laboratory of Biohydrometallurgy, Ministry of Education,
School of Minerals Processing and Bioengineering, Central South University, Changsha 410083, China

Received 18 October 2019; accepted 6 April 2020

Abstract: The effects of visible light and Cd^{2+} ion on chalcopyrite bioleaching in the presence of *Acidithiobacillus ferrooxidans* (*A. ferrooxidans*) were studied by scanning electron microscopy (SEM), synchrotron radiation X-ray diffraction (SR-XRD), and X-ray photoelectron spectroscopy (XPS). The results of bioleaching after 28 days showed that the copper dissolution increased by 4.96% with only visible light, the presence of Cd^{2+} alone exerted slight inhibition effect on chalcopyrite dissolution and the concentration of dissolved copper increased by 14.70% with visible light and 50 mg/L Cd^{2+}. The results of chemical leaching showed that visible light can promote the circulation of iron. SEM results showed that Cd^{2+} promoted the attachment of *A. ferrooxidans* on chalcopyrite surface under visible light. SR-XRD and XPS results indicated that visible light and Cd^{2+} promoted chalcopyrite dissolution, but did not inhibit the formation of passivation. Finally, a model of synergistic catalysis mechanism of visible light and Cd^{2+} on chalcopyrite bioleaching was proposed.

Key words: bioleaching; chalcopyrite; Cd^{2+}; *Acidithiobacillus ferrooxidans*; visible light

1 Introduction

Chalcopyrite is the most abundant copper-bearing mineral, which accounts for about 70% of the world's copper resources [1,2]. Currently, the most common method for recovering copper from chalcopyrite is pyrometallurgy. However, most pyrometallurgy processes emit polluted gases (primarily SO_2) and are expensive [3]. Bioleaching is often used to extract metals from low-grade ores [4] with the advantages of easy operation, mild reaction conditions, environment friendliness and low energy consumption [5,6]. Accordingly, bioleaching has been proposed to recover copper from chalcopyrite. However, chalcopyrite is challenging to bioleaching due to its high lattice energy and strong passivation effect [7,8].

A lot of efforts have been made to understand the chalcopyrite bioleaching mechanism and enhance the process of chalcopyrite bioleaching. For instance, bioleaching experiments have been performed using mesophilic mixed cultures mutated by ultrasound and microwaves [9], mixed thermophilic bacteria [10], metal ion catalysts [11], varied temperatures and pH [12], activated carbon [13] and nonionic surfactant [14]. Various metal ions, such as Ag^+ [15,16], Fe^{2+} [17], Hg^{2+} [18], Bi^{3+} [19], Cu^{2+} [20] and Co^{2+} [11], have been used to promote bioleaching process. Among these metal ions, great attentions have been paid to the silver ion. The main reason for the chalcopyrite bioleaching catalyzed by silver ion is the formation of silver-containing intermediate products such as silver sulfide and metallic silver [21]. However, high cost of silver hindered its industrial application.

Foundation item: Projects (51774332, 51934009, 51704331, 51804350, U1932129) supported by the National Natural Science Foundation of China; Project (2018JJ1041) supported by the Natural Science Foundation of Hunan Province, China
Corresponding author: Jun WANG, Tel: +86-731-88876557, E-mail: wjwq2000@126.com
DOI: 10.1016/S1003-6326(20)65279-7

Compared with silver ion, cadmium ion (Cd^{2+}) is a kind of heavy-metal ion, which is abundant, inexpensive, and widely present in polluted water and soil [22,23]. LIU and co-workers proposed that low concentration of Cd^{2+} can promote the growth of bacteria, because Cd^{2+} can be adsorbed on the cell surface, which made the cell permeability increased and nutrition was easily absorbed [24]. It has been reported that some bacteria can induce Cd^{2+} to form CdS nanoparticles [25]. SAKIMOTO et al [26] have shown that CdS nanoparticles can be used as light harvester to maintain cellular metabolism of the nonphotosynthetic bacterium. Also, *Acidithiobacillus ferrooxidans (A. ferrooxidans)* contains cadmium resistant genes [27,28], which can maintain metabolic activity in high concentrations (5−100 mmol/L) of Cd^{2+} [22,29].

On the other hand, chalcopyrite bioleaching is also affected by its semiconducting property [30]. In recent years, some researchers have proven that based on the semiconducting property of chalcopyrite, visible light can promote the chalcopyrite biodissolution efficiency [31−33]. Concretely speaking, the photoelectrons produced when the chalcopyrite were excited by visible light can reduce Fe^{3+} to Fe^{2+}, which is the metabolic substrate for *A. ferrooxidans*, and can effectively promote the growth of bacteria and thus benefits chalcopyrite bioleaching [31].

However, to date, the synergistic effect of visible light and Cd^{2+} on bioleaching has not been reported. Therefore, the purposes of this study were to: (1) discuss the synergistic effects of visible light and Cd^{2+} on chalcopyrite bioleaching, (2) investigate the mechanism of visible light and Cd^{2+} on chalcopyrite bioleaching. Synchrotron radiation X-ray diffraction (SR-XRD), scanning electron microscopy (SEM) and X-ray photoelectron spectroscopy (XPS) were used to examine the changes of chalcopyrite surface morphology, phase and element to better understand the roles of visible light and cadmium ion in chalcopyrite bioleaching.

2 Experimental

2.1 Chalcopyrite and *A. ferrooxidans* culture preparation

Chalcopyrite sample was obtained from Guangzhou, Guangdong Province, China. X-ray fluorescence (XRF) spectroscopic analysis showed that the untreated chalcopyrite sample contained the following elements (wt.%): Cu, 33.21; S, 31.59; Fe, 28.21; O, 4.88; Al, 0.052; Si, 0.837; Mg, 0.202; Ca, 0.924; Mn, 0.014; Co, 0.0131; Zn, 0.0273; Se, 0.0169; Sr, 0.004 and Ag, 0.022. In order to accurately determine the content of copper in chalcopyrite sample, chemical analysis (iodometric titration) was carried out, and it was found that the content of copper was 32.49 wt.% [34] in the sample. The SR-XRD results (Fig. 1) revealed the high purity of the chalcopyrite used in this study. The untreated chalcopyrite was ground to obtain fine particles of 74 μm or less.

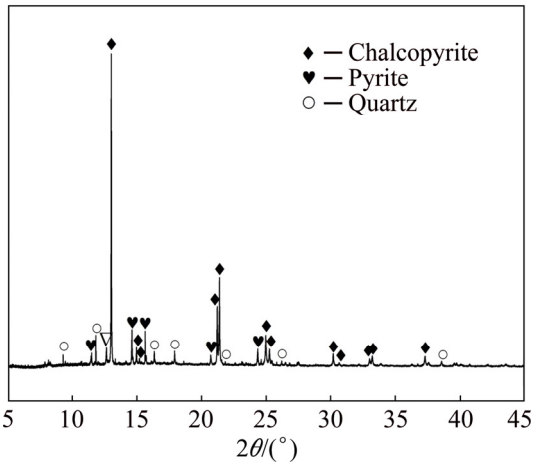

Fig. 1 SR-XRD pattern of chosen sample of chalcopyrite

A. ferrooxidans strain (ATCC 23270) applied for the following experiments was obtained from American Type Culture Collection [35]. *A. ferrooxidans* was cultured in the medium 9K comprising of 3 g/L of $(NH_4)_2SO_4$, 0.1 g/L of KCl, 0.5 g/L of $K_2HPO_4{\cdot}3H_2O$, 0.5 g/L of $MgSO_4{\cdot}7H_2O$, 0.01 g/L of $Ca(NO_3)_2$ and 44.7 g/L of $FeSO_4{\cdot}7H_2O$. pH was controlled to be 2.0 approximately with H_2SO_4 (0.01 mol/L) and/or NaOH (0.01 mol/L) [29]. The cells were harvested during the exponential growth phase after being subcultured three times (30 °C, 170 r/min). The cell suspension was filtered with Whatman 42 filter paper [33], and the filtrate was transferred into 200 mL sterilized centrifuge bottles and centrifuged at 10000 r/min for 15 min to collect cells. The isolated bacteria were collected and placed in iron-free 9K medium and centrifuged again (12000 r/min, 2 min). The above steps

were repeated three times to remove iron ions. Since iron ions are important to dissolve chalcopyrite [17], which have a great influence on our experiments.

2.2 Experimental settings

Two experimental systems were set up and labelled as 'BioL' and 'ChemL-Fe' (Table 1). All experiments were performed in 250 mL Erlenmeyer flasks containing 100 mL of sterilized 9K medium. The original pH of the 9K medium was controlled to be 2.0 using 0.1 mol/L H_2SO_4 and/or 0.01 mol/L NaOH. Each Erlenmeyer flask was filled with 2 g of chalcopyrite and placed on a rotary shaker at 30 °C and 170 r/min [15,31,36]. The effects on leaching efficiency under visible light and darkness conditions were studied. In bioleaching systems, 2 mL of bacteria cultures were added to each Erlenmeyer flask to ensure that the original cell concentration exceeded 1.0×10^7 cells/mL [35]. Afterwards, different Cd^{2+} (cadmium sulphate) concentrations (0, 25, 50, 75 and 100 mg/L) were added. The 'ChemL-Fe' system was adopted under the condition of Cd^{2+} (0 and 50 mg/L), 0.1 mol/L Fe^{3+} (iron sulphate) and without bacteria [31]. The details of these systems are given in Table 1. All experiments were repeated thrice to ensure reliability. Distilled water was periodically added to the system to compensate for evaporation loss. Aliquots collected for sample analysis were supplemented by sterile 9 K medium.

2.3 Analysis methods

2.3.1 Leaching parameters

About 200 μL of supernatant was collected from each Erlenmeyer flask every 3 days to determine cell densities and the concentrations of Cu^{2+}, Fe^{2+} and total iron (TFe). Changes in pH and redox potential (vs. Ag/AgCl) were simultaneously measured. The concentrations of copper ions was determined by BCO spectrophotometry. The concentration of Fe^{2+} and TFe were measured by byo-phenanthroline spectrophotography [33]. The number of free cells was measured by optical microscopy (CX31) [35].

At the initial 20, 40, 60, 80 and 100 min of bioleaching, 10 μL supernatant was taken respectively to determine the free cell density. Then, the adsorption rate (Q) was calculated by the following formula:

$$Q=(C_0-C)/C_0\times100\% \quad (1)$$

where C_0 and C represent the initial cell concentration and the free cell concentration, respectively [35].

2.3.2 Surface feature

The leaching residues of each conical flask were passed through filter paper, washed with sterile water, and dried in a vacuum-drying oven (DZF−6050). A portion of the sample was removed from the vacuum oven, sprayed with gold and placed in SEM (Nova^{TM} NanoSEM 230, FEI, USA) chamber for morphology analysis.

2.3.3 Composition of leaching residues

The filtered samples were rinsed with distilled water and placed in a vacuum oven to prevent oxidation. The composition of the bioleaching residues was analyzed by SR-XRD at the beam line BL14B1 of the Shanghai Synchrotron Radiation Facility (China). The wavelength used was 0.6887 Å. The filter residues in the two chemical leaching systems were dried for XRD analysis. XPS testing was performed using ESCALAB 250Xi. The spectrum was noted with Al K_α X-ray source and a constant pass energy of 20 eV (0.1 eV/step). The binding energies were referred to the C 1s level at 284.6 eV [37]. Given the splitting of the spin orbit, the S 2p peaks were divided into the S $2p_{3/2}$ and S $2p_{1/2}$ peaks. The intensity of the S $2p_{3/2}$ peak for the same species was twice that of the S $2p_{1/2}$ peak, and the binding energy of the $2p_{3/2}$ peak was 1.19 eV higher. The background of the spectrum was based on the Shirley method [38].

Table 1 Experiment parameters for bioleaching and chemical leaching systems

System	Bacteria	$[Fe^{3+}]$/(mol·L^{-1})	$[Cd^{2+}]$/(mg·L^{-1})	Visible light	Chalcopyrite/g	Solution volume/mL
BioL	*A. f*	−	0, 25, 50, 75, 100	+/−	2.0	100
ChemL-Fe	−	0.1	0, 50	+/−	2.0	100

'–' means absence; '+' means existence; *A. f* means *A. ferrooxidans*

3 Results and discussion

3.1 Bioleaching behavior

The synergistic effects of Cd^{2+} and visible light on chalcopyrite bioleaching were investigated. The effects of varied Cd^{2+} concentrations (0, 25, 50, 75 and 100 mg/L) on chalcopyrite bioleaching were explored, and results showed that the catalytic effect was the best at 50 mg/L Cd^{2+}. Specifically, the copper extraction concentrations were (3.58±0.02), (3.71±0.01), (3.91±0.02), (3.79±0.02) and (3.65±0.02) g/L for 0, 25, 50, 75 and 100 mg/L Cd^{2+}, respectively, after 28 days of bioleaching under the visible light. Thus, focus was given on the effect of 50 mg/L Cd^{2+} on chalcopyrite bioleaching. As shown in Fig. 2(a), the dissolved copper slowly increased in the first 6 days primarily because of the low concentration of *A. ferrooxidans*. The chalcopyrite dissolution rate increased on the 6th

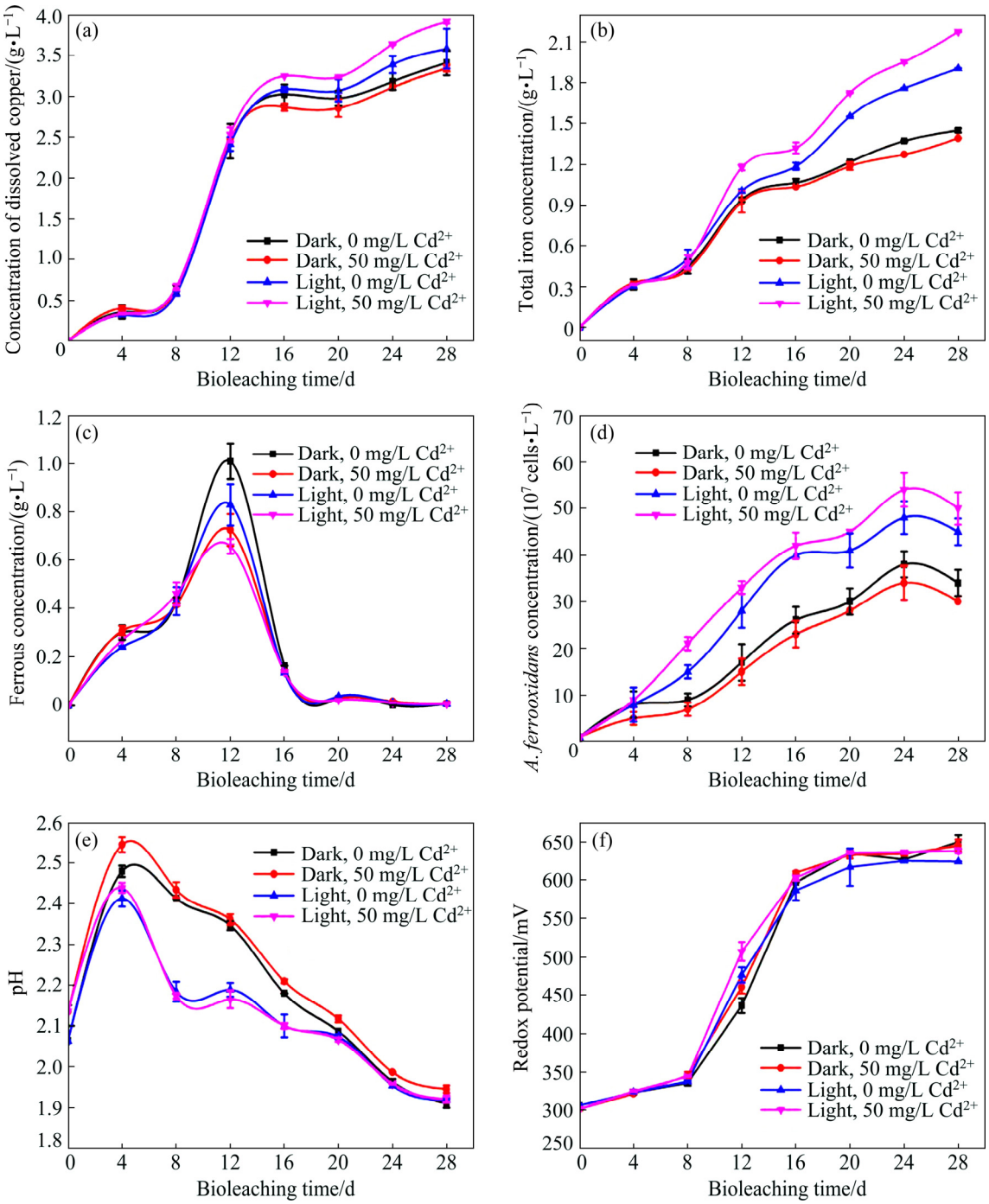

Fig. 2 Changes in concentration of dissolved copper (a), total iron concentration (b), ferrous concentration (c), *A. ferrooxidans* concentration (d), pH (e) and redox potential (f), during bioleaching of chalcopyrite by *A. ferrooxidans*

day and then decreased after the 14th day. The low leaching rate may be attributed to passivation-layer inhibition. Finally, at 0 and 50 mg/L Cd^{2+}, the copper extraction concentrations under visible light were (3.58±0.02) and (3.91±0.01) g/L, respectively. By comparison, at 0 and 50 mg/L Cd^{2+}, the dissolved copper concentrations in the bioleaching system without visible light were (3.41±0.11) and (3.34±0.03) g/L, respectively. The concentration of dissolved copper increased by 4.96% only in the presence of visible light. When visible light and 50 mg/L Cd^{2+} were both present, the dissolution rate of copper was the highest, i.e., 14.70% higher. These results showed that the presence of visible light increased the chalcopyrite bioleaching rate. Based on Fig. 2(a), a conclusion can be drawn that Cd^{2+} inhibited chalcopyrite bioleaching in darkness but promoted it under visible light.

Figures 2(b) and 2(c) showed the trends of TFe and Fe^{2+} concentrations. The concentration of TFe progressively increased. Under visible light and 50 mg/L Cd^{2+}, the concentration of total iron was the highest, which is mainly due to the oxidation and dissolution of chalcopyrite (Eqs. (2) and (3)) [32]. Ferrous ions produced by chalcopyrite dissolution were oxidized by *A. ferrooxidans* to iron ions (Eq. (4)), which in turn promoted the oxidative decomposition of chalcopyrite (Eq. (2)). By contrast, the concentration of ferrous ions rapidly decreased on the 12th day and remained at a low level. These phenomena were due to the fact that bacteria grew rapidly, which made the rate of ferrous oxidation by bacteria faster than that of the dissolution of chalcopyrite. Under visible light, the concentration of ferrous ions was low and the concentration of total iron was high, which was mainly due to the photocatalytic reaction on the chalcopyrite surface that promoted the growth of bacteria and accelerated ferrous oxidation [33]. Some researchers have found that cadmium sulphide particles formed on bacterial surfaces through sedimentation can capture photogenerated electrons and promote the utilization of photogenerated electrons [26,39]. The growth of bacteria promoted the transformation of ferrous ions into iron ions (Eq. (4)). Accordingly, under light conditions, the group with Cd^{2+} had the highest total iron concentration, the highest cell concentration and the lowest ferrous concentration (Figs. 2(b) and 2(d), respectively). These results indicated that Cd^{2+} improved the photogenerated electron transfer and its utilization efficiency, promoted the growth of *A. ferrooxidans* in the presence of visible light and improved the photocatalytic efficiency of chalcopyrite bioleaching.

$$CuFeS_2+4Fe^{3+} \rightarrow Cu^{2+}+5Fe^{2+}+2S^0 \quad (2)$$

$$CuFeS_2+4H^++O_2 \rightarrow Cu^{2+}+Fe^{2+}+2S^0+2H_2O \quad (3)$$

$$4Fe^{2+}+4H^++O_2 \xrightarrow{A.f} 4Fe^{3+}+2H_2O \quad (4)$$

Figure 2(e) showed the changes in solution pH during chalcopyrite bioleaching. The pH initially increased, decreased on the fourth day and finally decreased to below 1.9. The increase in pH was mainly due to the consumption of hydrogen ions by chalcopyrite dissolution (Eq. (3)), whereas the decrease meant that acid was produced by the oxidation of elemental sulphur by *A. ferrooxidans* (Eq. (5)) and the formation of jarosite (Eq. (6)) [33]. Under visible light, the pH values of the bioleaching system were lower than those in darkness. The pH value was the lowest when Cd^{2+} was added. When cadmium and visible light were both present, the pH drop was very pronounced mainly because of the massively growth of *A. ferrooxidans* (Eq. (5)) and the formation of jarosite (Eq. (6)) [36]:

$$2S^0+3O_2+2H_2O \xrightarrow{A.f} 2SO_4^{2-}+4H^+ \quad (5)$$

$$M^++3Fe^{3+}+2SO_4^{2-}+6H_2O \rightarrow MFe_3(SO_4)_2(OH)_6+6H^+ \quad (6)$$

where M may be K^+, NH_4^+, H_3O^+ or Na^+.

The effects of visible light and Cd^{2+} on redox potential are shown in Fig. 2(f). Redox potential is an important factor in the leaching process of chalcopyrite, which is mainly related to the ratio of $[Fe^{3+}]/[Fe^{2+}]$ and $[H^+]$ in the solution [40]. In this study, redox potential increased slowly in the first 8 days, then rapidly increased from the 8th to the 16th day until it reached >600 mV (vs Ag/AgCl) and finally remained unchanged during chalcopyrite bioleaching. The increase of redox potential in the first 8 days was mainly related to the oxidation of ferrous ions by *A. ferrooxidans* (Eq. (4)), which indicated that the redox potential was mainly affected by $[Fe^{3+}]/[Fe^{2+}]$ [31,33]. The redox potential of each group was almost the same. From the 8th to the 16th day, compared with the dark group, the redox potential of the light group was

relatively high. The rise of redox potential was related to the rapid decline of pH value in this stage, and the difference between light group and dark group was also consistent with the difference of pH values. At this time, redox potential is mainly affected by [H^+] [40]. Finally, the redox potential remained almost unchanged, which was consistent with the change of ferrous ion concentration.

The adsorption rate of *A. ferrooxidans* on chalcopyrite in the first 100 min of bioleaching is shown in Fig. 3. Under dark conditions, the addition of Cd^{2+} slightly inhibited the adsorption of *A. ferrooxidans* on chalcopyrite surface; while under visible light, Cd^{2+} promoted the attachment of *A. ferrooxidans* to chalcopyrite. Microorganisms can only utilize insoluble mineral substrates after they attached to the mineral surface [41]. Therefore, the attachment of *A. ferrooxidans* to chalcopyrite surface is the key step in the bioleaching of chalcopyrite.

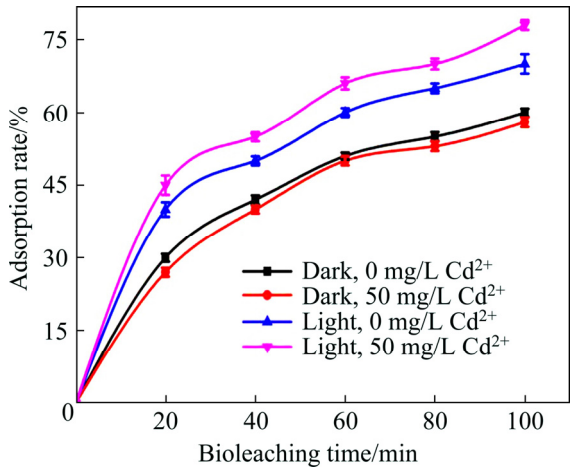

Fig. 3 Variation of adsorption rate of *A. ferrooxidans*

According to the above analysis, visible light and Cd^{2+} accelerated chalcopyrite bioleaching by accelerating the cycling of iron and ferrous ions, increasing the concentration of *A. ferrooxidans*, reducing the pH value and promoting the attachment of *A. ferrooxidans* to chalcopyrite.

3.2 SEM analysis of surface feature

The surface characteristics of chalcopyrite ore and leaching residues analyzed by SEM are shown in Fig. 4. The surface of the untreated chalcopyrite was flat (Fig. 4(a)). After chemical leaching, the chalcopyrite surface changed slightly in light and darkness whether or not Cd^{2+} was added (Figs. 4(b)−(e)). The chalcopyrite surface was eroded by *A. ferrooxidans* after bioleaching and became more complex than that after chemical leaching (Figs. 4(f)–(i)). Figures 4(f) and 4(h) showed that under dark conditions, a small amount of *A. ferrooxidans* bacteria can be found on the chalcopyrite surface without Cd^{2+} and are about 2.0 μm long and 0.5 μm wide, whereas no bacteria can be found on the mineral surface with 50 mg/L Cd^{2+}. This is because the toxicity of cadmium ion limited the reproduction of *A. ferrooxidans* [22]. Under visible-light conditions, some membranous substances were found on the chalcopyrite surface without Cd^{2+} and were presumed as extracellular polymeric substance (EPS), whereas a large number of *A. ferrooxidans* bacteria adsorbed onto the chalcopyrite surface with 50 mg/L Cd^{2+} (Figs. 4(g) and 4(i)). Attached biomass was increased and further increased free biomass [42], which is consistent with the conclusion of Fig. 2(d). This phenomenon indicated that under visible light, Cd^{2+} promoted chalcopyrite bioleaching by promoting the attachment of *A. ferrooxidans* to chalcopyrite surface. The attachment of bacteria to chalcopyrite surface and the production of EPS played an important role in chalcopyrite bioleaching [7,43]. The attachment of *A. ferrooxidans* to chalcopyrite surface was the first step of bioleaching. The interface between bacteria and minerals provided space for bioleaching reactions [43]. EPS produced by bacteria can form a high oxidation activity area near the chalcopyrite surface by accumulating Fe^{3+}, thus enhancing dissolution of chalcopyrite [44,45]. In turn, the dissolution of chalcopyrite released energy materials, such as elemental sulfur and ferrous iron, which made the attached cells proliferate rapidly [46]. This is consistent with the conclusion of Figs. 2(a) and 2(d).

3.3 SR-XRD analysis of chalcopyrite residues

SR-XRD analysis indicated that chalcopyrite, elemental sulphur and jarosite were the main components of chalcopyrite-bioleaching residue (Fig. 5). The SR-XRD results of bioleaching residue in darkness showed that the characteristic peaks of chalcopyrite were obvious, whereas those of chalcopyrite from bioleaching residue under light conditions were relatively low. As such, the chalcopyrite content was low. However, the characteristic peaks of elemental sulphur and

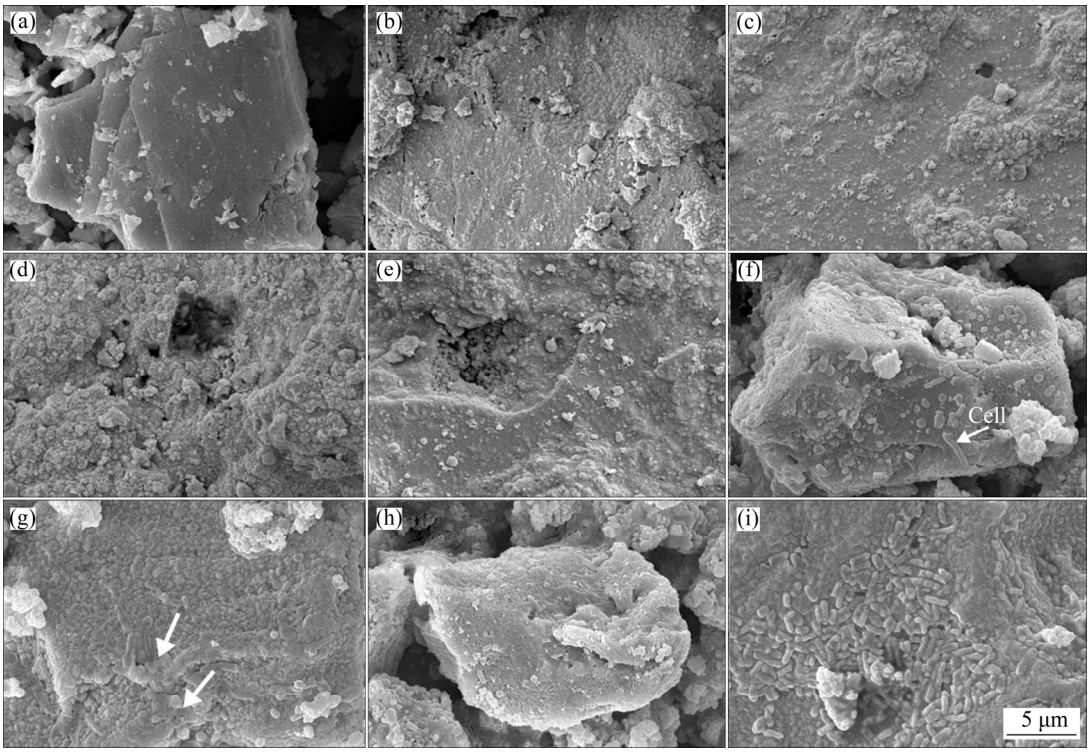

Fig. 4 SEM images of original chalcopyrite (a), chemical leaching residues (b−e) and bioleaching residues (f−i): (b, f) Dark, 0 mg/L Cd^{2+}; (c, g) Light, 0 mg/L Cd^{2+}; (d, h) Dark, 50 mg/L Cd^{2+}; (e, i) Light, 50 mg/L Cd^{2+}

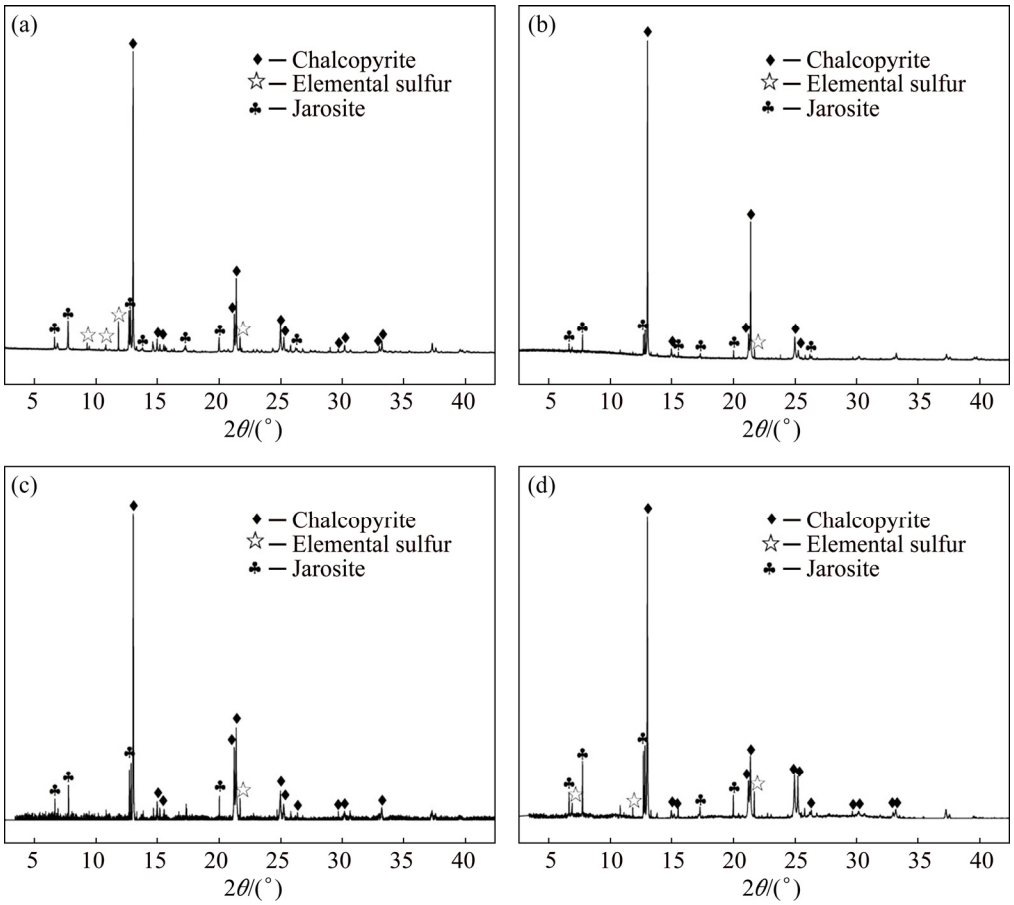

Fig. 5 SR-XRD patterns of chalcopyrite residues leached by *A. ferrooxidans*: (a) Dark, 0 mg/L Cd^{2+}; (b) Light, 0 mg/L Cd^{2+}; (c) Dark, 50 mg/L Cd^{2+}; (d) Light, 50 mg/L Cd^{2+}

jarosite were obvious under visible light, indicating that the contents of both substances had increased. This result combined with that shown in Fig. 2 suggested that adding Cd^{2+} to the visible light system of bioleaching significantly promoted chalcopyrite dissolution. However, the inhibitory effect on the formation of passivating components (jarosite and elemental sulphur) was not obvious.

3.4 Surface species determined by XPS

The chemical formula of chalcopyrite is $Cu^{+}Fe^{3+}(S^{2-})_2$, in which the elemental sulphur has a valence of −2 [37,47]. Polysulphide (S_n^{2-}), elemental sulphur (S^0) and sulphate (jarosite, SO_4^{2-}) were the main components of the passivation layer [48−50]. In this work, we primarily studied the existence of S 2p peaks on the chalcopyrite leaching slags surface (Fig. 6 and Table 2). Sulphur

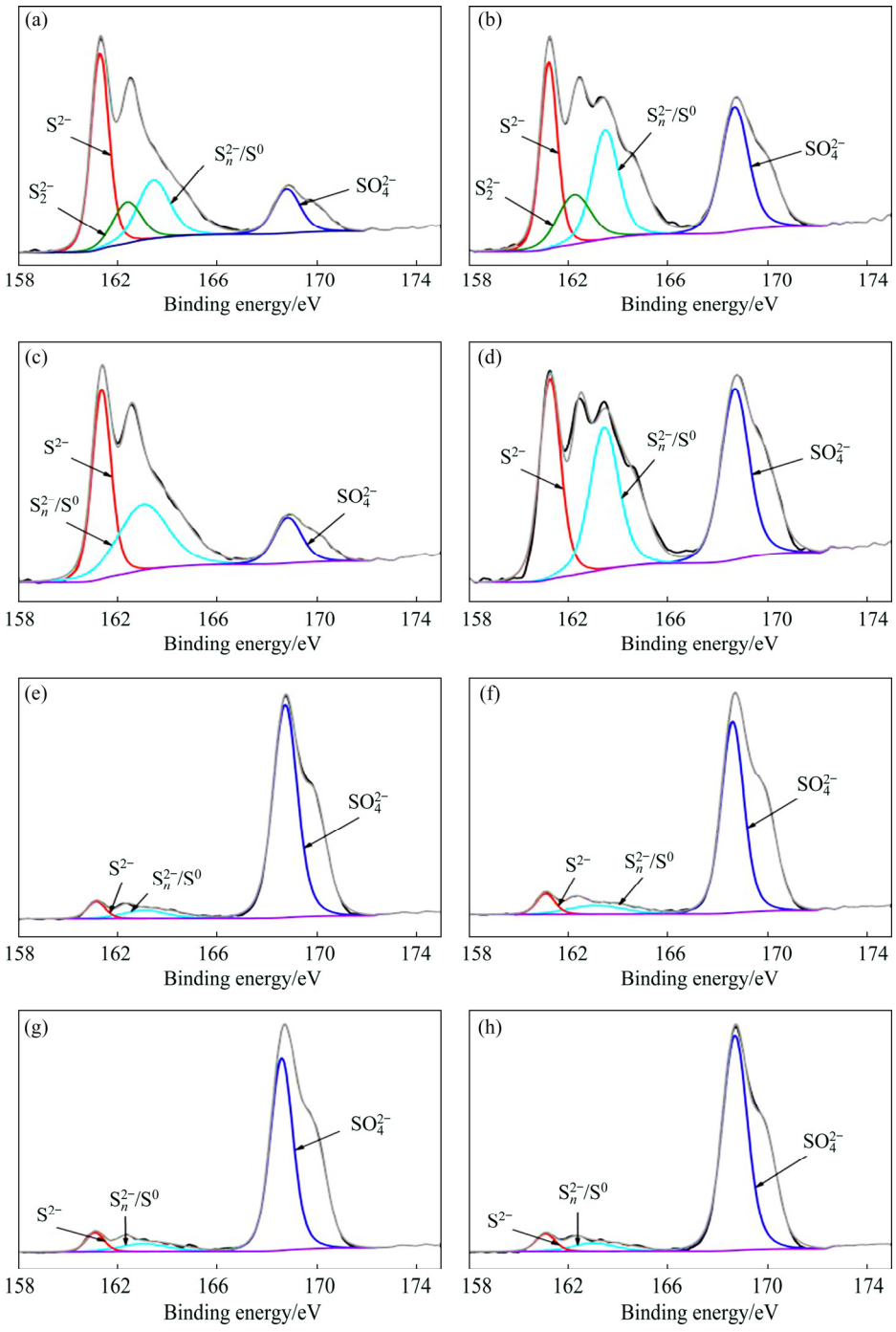

Fig. 6 XPS spectra of S 2p peaks of chemical leaching residues (a−d) and bioleaching residues (e−h): (a, e) Dark, 0 mg/L Cd^{2+}; (b, f) Light, 0 mg/L Cd^{2+}; (c, g) Dark, 50 mg/L Cd^{2+}; (d, h) Light, 50 mg/L Cd^{2+}

Table 2 Contents of different sulphur species in sulfur layer of chalcopyrite (at.%)

Sample	S^{2-}	S_2^{2-}	S_n^{2-}/S^0	SO_3^{2-}	SO_4^{2-}
BioL 0H	5.18	−	6.08	−	88.73
BioL 0G	6.27	−	7.80	−	85.92
BioL 50H	6.12	−	5.72	−	88.16
BioL 50G	5.72	−	6.12	−	88.16
ChemL-Fe 0H	45.51	15.07	24.27	−	15.15
ChemL-Fe 0G	28.64	14.91	26.03	−	30.42
ChemL-Fe 50H	45.75	−	41.34	−	12.91
ChemL-Fe 50G	32.47	−	31.33	−	36.20

0H—Dark, 0 mg/L Cd^{2+}; 0G—Light, 0 mg/L Cd^{2+}; 50H—Dark, 50 mg/L Cd^{2+}; 50G—Light, 50 mg/L Cd^{2+}

species were primarily classified into six types: monosulphide (S^{2-}, binding energy 161.1−161.8 eV, FWHM 0.5−0.7 eV), disulphide (S_2^{2-}, binding energy 162.3−162.4 eV, FWHM 0.5−0.7 eV), polysulphide (S_n^2, binding energy 163.0−163.9 eV, FWHM 1.1−1.3 eV), elemental sulphur (S^0, binding energy 163.05−164.7 eV, FWHM 0.7−1.7 eV), sulphite (SO_3^{2-}, binding energy 166.4−166.5 eV), and sulphate (SO_4^{2-}, binding energy 168.0−169.0 eV, FWHM 0.9 eV) [51−53]. The binding energies and relative contents of sulphur species are listed in Table 2. The contents of S^{2-}, S_2^{2-}, S_n^{2-}/S^0 and SO_4^{2-} were calculated from the area under the S 2p peak [53]. In the bioleaching processes, visible light was found to increase the content of S_n^{2-}/S^0, whereas adding Cd^{2+} reduced the content of S^{2-}. In the Cheml-Fe groups, the light system produced more SO_4^{2-} and less S_n^{2-}/S^0 than those of the dark system, indicating that chalcopyrite decomposed more thoroughly and produced more jarosite in light than in darkness.

3.5 Effects of visible light and Cd^{2+} on chalcopyrite leaching with Fe^{3+}

A series of experiments was carried out (Table 1, ChemL-Fe) to clarify the direct effects of visible light and Cd^{2+} on iron cycling in the chemical leaching system. The results in Fig. 7 indicated that the concentrations of total iron and ferrous in the visible system were higher than those in the dark system. As shown in Fig. 7(a), the concentration of dissolved copper was the highest in the presence of visible light, but adding Cd^{2+} had no obvious promotion effect on chalcopyrite leaching by Fe^{3+}. Under visible light, the concentration of ferrous ions in the solution was relatively high, which may be attributed to the promotion of Fe^{3+} reduction and corresponding production of more Fe^{2+} ions caused by the photoelectron light generated in the chalcopyrite. Moreover, a higher concentration of Fe^{2+} ions and lower concentration of Fe^{3+} in the system of light led to lower redox potential, which is determined by the ratio of Fe^{3+}/Fe^{2+}, thereby promoting the dissolution of chalcopyrite [54−56]. This phenomenon promoted the further release of iron. In conclusion, light played a key role in maintaining the chemical cycle of iron and improving chalcopyrite leaching, whereas Cd^{2+} had no effect on chalcopyrite leaching.

3.6 Proposed mechanism model

Based on the above analyses, the mechanism of visible light and Cd^{2+} enhancing chalcopyrite bioleaching is shown in Fig. 8. Chalcopyrite possesses an electronic structure composed of a valence band (VB) and a conduction band (CB). By absorbing photons with energy equal to or greater than the band-gap energy, the valence band electrons (e) can be excited to the conduction band. Then, the electrons migrate to the surface of chalcopyrite and promote the conversion of Fe^{3+} to Fe^{2+}. In addition, in visible light, Cd^{2+} can strengthen the adsorption of bacteria onto chalcopyrite surface, thus promoting chalcopyrite bioleaching. The possible reasons why Cd^{2+} promoted the attachment of *A. ferrooxidans* on chalcopyrite surface under visible light are as follows. (1) The low concentration of Cd^{2+} can increase the permeability of cell membrane and make the absorption of nutrients more easily [24]. Visible light promotes the circulation of iron, produces more Fe^{2+} for *A. ferrooxidans*, thus promoting the growth of bacteria. Therefore, when visible light and Cd^{2+} exist at the same time, there will be a large number of bacteria adsorbed on the mineral surface. (2) Bacteria induce Cd^{2+} to form CdS nanoparticles [25], which can be used as light collectors to maintain the cell metabolism of non-photosynthetic bacteria [26], thus promoting the growth and adsorption of bacteria. (3) Cd^{2+} can improve the electrochemical activity of chalcopyrite, thus strengthening the bacterial adhesion on the chalcopyrite surface [35].

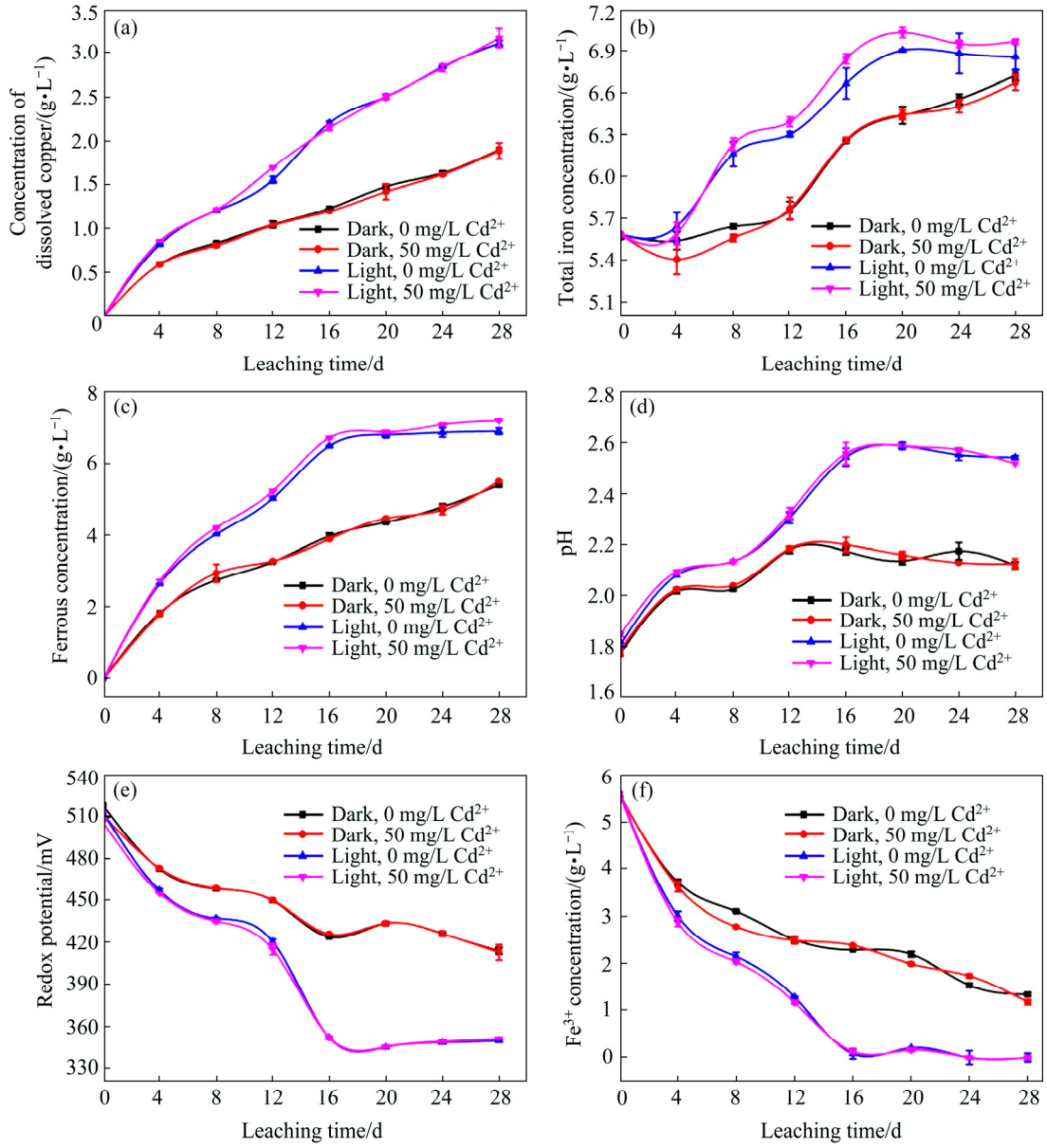

Fig. 7 Changes in concentration of dissolved copper (a), total iron concentration (b), ferrous concentration (c), pH (d), redox potential (e) and Fe^{3+} concentration (f) during leaching of chalcopyrite by Fe^{3+}

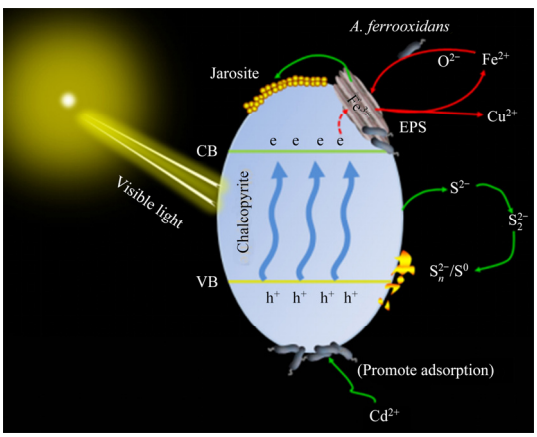

Fig. 8 Mechanism of visible light and Cd^{2+} enhancing chalcopyrite bioleaching

4 Conclusions

(1) Under visible light conditions, a low concentration (50 mg/L) of Cd^{2+} can strengthen the adsorption of bacteria onto the chalcopyrite surface and promote the growth of *A. ferrooxidans* to enhance chalcopyrite bioleaching.

(2) Visible light significantly influenced the promotion of the Fe^{3+}/Fe^{2+} cycle, and Fe^{2+} regeneration provided energy for *A. ferrooxidans*. In addition, visible light increased cell biomass and decreased redox potential and acidity, thereby promoting copper dissolution during chalcopyrite

bioleaching.

(3) Visible light and Cd^{2+} exerted a synergistic catalysis effect on chalcopyrite bioleaching in the presence of *A. ferrooxidans*. And the mechanism diagram of visible light and Cd^{2+} catalysis for chalcopyrite bioleaching was proposed.

Acknowledgments

The authors thank beamline BL14B1 (Shanghai Synchrotron Radiation Facility) for providing the beam time and help during experiments.

References

[1] CORDOBA E M, MUNOZ J A, BLAZQUEZ M L, GONZALEZ F, BALLESTER A. Leaching of chalcopyrite with ferric ion. Part I: General aspects [J]. Hydrometallurgy, 2008, 93: 81−87.

[2] ZHAO Hong-bo, ZHANG Yi-sheng, ZHANG Xian, QIAN Lu, SUN Meng-lin, YANG Yu, ZHANG Yan-sheng, WANG Jun, KIM H, QIU Guan-zhou. The dissolution and passivation mechanism of chalcopyrite in bioleaching: An overview [J]. Minerals Engineering, 2019, 136: 140−154.

[3] WATLING H R. Chalcopyrite hydrometallurgy at atmospheric pressure: 1. Review of acidic sulfate, sulfate–chloride and sulfate–nitrate process options [J]. Hydrometallurgy, 2013, 140: 163−180.

[4] WANG Jun, QIN Wen-qing, ZHANG Yan-sheng, YANG Cong-ren, ZHANG Jian-wen, NAI Shao-shi, SHANG He, QIU Guan-zhou. Bacterial leaching of chalcopyrite and bornite with native bioleaching microorganism [J]. Transactions of Nonferrous Metals Society of China, 2008, 18: 1468−1472.

[5] WANG Jun, ZHAO Hong-bo, ZHUANG Tian, QIN Wen-qing, ZHU Shan, QIU Guan-zhou. Bioleaching of Pb−Zn−Sn chalcopyrite concentrate in tank bioreactor and microbial community succession analysis [J]. Transactions of Nonferrous Metals Society of China, 2013, 23: 3758−3762.

[6] ZHANG Ming-jiang, CHEN Bo-wei, WANG Nan, CHEN Jing-he.; ZOU Lai-chang, LIU Xing-yu, WANG Zi-ning, WEN Jian-kang, LIU Wen-yan. Effects of heap-bioleaching plant on microbial community of the nearby river [J]. International Biodeterioration & Biodegradation, 2018, 128: 36−40.

[7] ZHU Jian-yu, WANG Qian-fen, ZHOU Shuang, LI Qian, GAN Min, JIANG Hao, QIN Wen-qing, LIU Xue-duan, HU Yue-hua, QIU Guan-zhou. Insights into the relation between adhesion force and chalcopyrite-bioleaching by *Acidithiobacillus ferrooxidans* [J]. Colloids and Surfaces B: Biointerfaces, 2015, 126: 351−357.

[8] QIN Wen-qing, YANG Cong-ren, LAI Shao-shi, WANG Jun, LIU Kai, ZHANG Bo. Bioleaching of chalcopyrite by moderately thermophilic microorganisms [J]. Bioresource Technology, 2013, 129: 200−208.

[9] ROYAEI M M, POURBABAEE A, NOAPARAST M. Copper recovery from chalcopyrite flotation concentrate using mixed mesophilic strains subjected to microwave and ultrasound irradiation [J]. Iranian Journal of Science and Technology, Transactions A: Science, 2018, 43: 335−343.

[10] WANG Yu-guang, SU Li-jun, ZHANG Li-juan, ZENG Wei-min, WU Jun-zi, WAN Li-li, QIU Guan-zhou, CHEN Xin-hua, ZHOU Hong-bo. Bioleaching of chalcopyrite by defined mixed moderately thermophilic consortium including a marine acidophilic halotolerant bacterium [J]. Bioresource Technology, 2012, 121: 348−354.

[11] PATHAK A, MORRISON L, HEALY M G. Catalytic potential of selected metal ions for bioleaching, and potential techno-economic and environmental issues: A critical review [J]. Bioresource Technology, 2017, 229: 211−221.

[12] YU Zhao-jing, YU Run-lan, LIU A-juan, LIU Jing, ZENG Wei-min, LIU Xue-duan, QIU Guan-zhou. Effect of pH values on extracellular protein and polysaccharide secretions of *Acidithiobacillus ferrooxidans* during chalcopyrite bioleaching [J]. Transactions of Nonferrous Metals Society of China, 2017, 27: 406−412.

[13] MA Ya-long, LIU Hong-chang, XIA Jin-lan, NIE Zhen-yuan, ZHU Hong-rui, ZHAO Yi-dong, MA Chen-yan, ZHENG Lei, HONG Cai-hao, WEN Wen. Relatedness between catalytic effect of activated carbon and passivation phenomenon during chalcopyrite bioleaching by mixed thermophilic Archaea culture at 65 °C [J]. Transactions of Nonferrous Metals Society of China, 2017, 27: 1374−1384.

[14] ZHANG Rui-yang, SUN Chun-bao, KOU Jue, ZHAO Hong-yu, WEI De-zhou, XING Yi. Enhancing the leaching of chalcopyrite using *Acidithiobacillus ferrooxidans* under the induction of surfactant Triton X-100 [J]. Minerals, 2019, 9: 11.

[15] NIE Zhen-yuan, ZHANG Wei-wei, LIU Hong-chang, XIA Jin-lan, ZHU Wei, ZHANG Duo-rui, ZHENG Lei, MA Chen-yan, ZHAO Yi-dong, WEN Wen. Synchrotron radiation based study of the catalytic mechanism of Ag^{+} to chalcopyrite bioleaching by mesophilic and thermophilic cultures [J]. Minerals, 2018, 8: 382.

[16] ZHAO Hong-bo, GAN Xiao-wen, WANG Jun, TAO Lang, QIN Wen-qing, QIU Guan-zhou. Stepwise bioleaching of Cu−Zn mixed ores with comprehensive utilization of silver-bearing solid waste through a new technique process [J]. Hydrometallurgy, 2017, 171: 374−386.

[17] LIU Huan, LU Xian-cai, ZHANG Li-juan, XIANG Wan-li, ZHU Xiang-yu, LI Juan, WANG Xiao-lin, LU Jian-jun, WANG Ru-cheng. Collaborative effects of *Acidithiobacillus ferrooxidans* and ferrous ions on the oxidation of chalcopyrite [J]. Chemical Geology, 2018, 493: 109−120.

[18] BALLESTER A, GONZALEZ F, BLAZQUEZ M L, MIER J L. The influence of various ions in the bioleaching of metal sulphides [J]. Hydrometallurgy, 1990, 23: 221−235.

[19] NIU Zhi-rui, HUANG Qi-fei, WANG Jia, YANG Yi-ran, XIN Bao-ping, CHEN Shi. Metallic ions catalysis for improving bioleaching yield of Zn and Mn from spent Zn-Mn batteries at high pulp density of 10% [J]. Journal of Hazardous Materials, 2015, 298: 170−177.

[20] MENG Xiao-yu, ZHAO Hong-bo, SUN Meng-lin, ZHANG Yi-sheng, ZHANG Yan-jun, LV Xin, KIM H, VAINSHTEIN M, WANG Shuai, QIU Guan-zhou. The role of cupric ions in

the oxidative dissolution process of marmatite: A dependence on Cu^{2+} concentration [J]. Science of the Total Environment, 2019, 675: 213−223.

[21] ZHAO Hong-bo, ZHANG Yi-sheng, SUN Meng-lin, OU Peng-fei, ZHANG Yan-jun, LIAO Rui, QIU Guan-zhou. Catalytic mechanism of silver in the oxidative dissolution process of chalcopyrite: Experiment and DFT calculation [J]. Hydrometallurgy, 2019, 187: 18−29.

[22] JAVIERA R Z, SEBASTIAN G, CRISTOBAL M B, RODRIGO N, CLAUDIO A N, ALBERTO P, CARLOS A J. Response of the biomining *Acidithiobacillus ferrooxidans* to high cadmium concentrations [J]. Journal of Proteomics, 2019, 198: 132−144.

[23] NIES D H. Microbial heavy-metal resistance [J]. Appl Microbiol Biotechnol, 1999, 51: 730−750.

[24] LIU Zheng, YANG Shao-bin, BAI Yu-shan, XIU Jin-jun, YAN Han, HUANG Jing, WANG Li-wei, ZHANG Hong-mei, LIU Ying. The alteration of cell membrane of sulfate reducing bacteria in the presence of Mn(II) and Cd(II) [J]. Minerals Engineering, 2011, 24: 839−844.

[25] WENDY J C, JOSEPH M S, RAJESH R N. Bio-directed synthesis and assembly of nanomaterials [J]. Chemical Society Reviews, 2008, 37: 2403−2412.

[26] SAKIMOTO K K, WONG A B, YANG Pei-dong. Self-photosensitization of nonphotosynthetic bacteria for solar-to-chemical production [J]. Science, 2016, 351: 74−77.

[27] ZHANG Yu, ZHANG Shuang, ZHAO Dan, NI Yong-qing, WANG Wei-dong, YAN Lei. Complete genome sequence of *Acidithiobacillus ferrooxidans* YNTRS-40, a strain of the ferrous iron- and sulfur-oxidizing acidophile [J]. Microorganisms, 2020, 8: 2.

[28] NIA O, RODRIGO N, CRISTOBAL M B, CLAUDIO A N, FERNANDO A, SERGIO A A, ALBERTO P, CARLOS A J. Possible role of envelope components in the extreme copper resistance of the biomining *Acidithiobacillus ferrooxidans* [J]. Genes, 2018, 9: 347.

[29] BAILLET F, MAGNIN J P, CHERUY A, OZIL P. Cadmium tolerance and uptake by a *Thiobacillus ferrooxidans* biomass [J]. Environmental Technology, 1997, 18: 631−638.

[30] ZHAO Hong-bo, HUANG Xiao-tao, WANG Jun, LI Yi-ni, LIAO Rui, WANG Xing-xing, QIU Xiao, XIONG Yu-ming, QIN Wen-qing, QIU Guan-zhou. Comparison of bioleaching and dissolution process of p-type and n-type chalcopyrite [J]. Minerals Engineering, 2017, 109: 153−161.

[31] ZHOU Shuang, GAN Min, ZHU Jian-yu, LI Qian, JIE Shi-qi, YANG Bao-jun, LIU Xue-duan. Catalytic effect of light illumination on bioleaching of chalcopyrite [J]. Bioresource Technology, 2015, 182: 345−352.

[32] YANG Bao-jun, LIN Mo, FANG Jing-hua, ZHANG Rui-yong, LUO Wen, WANG Xing-xing, LIAO Rui, WU Bai-qiang, WANG Jun, GAN Min, LIU Bin, ZHANG Yi, LIU Xue-duan, QIN Wen-qing, QIU Guan-zhou. Combined effects of jarosite and visible light on chalcopyrite dissolution mediated by *Acidithiobacillus ferrooxidans* [J]. Science of the Total Environment, 2020, 698: 134175.

[33] YANG Bao-jun, GAN Min, LUO Wen, ZHOU Shuang, LEI Pan, ZENG Jian, SUN Wei, ZHU Jian-yu, HU Yue-hua. Synergistic catalytic effects of visible light and graphene on bioleaching of chalcopyrite [J]. RSC Advances, 2017, 7: 49838−49848.

[34] PANOSSIAN Z, FERRARI J V, ALMEIDA M B. Determination of copper and zinc contents in brass plating solutions by titrimetric analysis: A review [J]. Plating & Surface Finishing, 2004, 91: 38−43.

[35] YANG Bao-jun, ZHAO Chun-xiao, LUO Wen, LIAO Rui, GAN Min, WANG Jun, LIU Xue-duan, QIU Guan-zhou. Catalytic effect of silver on copper release from chalcopyrite mediated by *Acidithiobacillus ferrooxidans* [J]. Journal of Hazardous Materials, 2020, 392: 122290.

[36] XIA Jin-lan, SONG Jian-jun, LIU Hong-chang, NIE Zhen-yuan, SHEN Li, YUAN Peng, MA Chen-yan, ZHENG Lei, ZHAO Yi-dong. Study on catalytic mechanism of silver ions in bioleaching of chalcopyrite by SR-XRD and XANES [J]. Hydrometallurgy, 2018, 180: 26−35.

[37] WANG Jun, GAN Xiao-wen, ZHAO Hong-bo, HU Ming-hao, LI Kai-yun, QIN Wen-qing, QIU Guan-zhou. Dissolution and passivation mechanisms of chalcopyrite during bioleaching: DFT calculation, XPS and electrochemistry analysis [J]. Minerals Engineering, 2016, 98: 264−278.

[38] ZHAO Hong-bo, WANG Jun, GAN Xiao-wen, HU Ming-hao, ZHANG Er-xing, QIN Wen-qing, QIU Guan-zhou. Cooperative bioleaching of chalcopyrite and silver-bearing tailing by mixed moderately thermophilic culture: An emphasis on the chalcopyrite dissolution with XPS and electrochemical analysis [J]. Minerals Engineering, 2015, 81: 29−39.

[39] KELSEY K S, STEPHANIE J Z, YANG Pei-dong. Cysteine-cystine photoregeneration for oxygenic photosynthesis of acetic acid from CO_2 by a tandem inorganic-biological hybrid system [J]. Nano Letters, 2016, 16: 5883−5887.

[40] DENG Sha, GU Guo-hua, XU Bao-ke, LI Li-juan, WU Bi-chao. Surface characterization of arsenopyrite during chemical and biological oxidation [J]. Science of the Total Environment, 2018, 626: 349−356.

[41] LI Ling-ling, LV Zao-sheng, YUAN Xiang-li. Effect of L-glycine on bioleaching of collophanite by *Acidithiobacillus ferrooxidans* [J]. International Biodeterioration & Biodegradation, 2013, 85: 156−165.

[42] FENG Shou-shuai, YANG Hai-lin, WANG Wu. Insights into the enhancement mechanism coupled with adapted adsorption behavior from mineralogical aspects in bioleaching of copper-bearing sulfide ore by *Acidithiobacillus* sp [J]. RSC Advances 2015, 5: 98057−98066.

[43] LIU Rong-hui, CHEN Jing, ZHOU Wen-bo, CHENG Hai-na, ZHOU Hong-bo. Insight to the early-stage adsorption mechanism of moderately thermophilic consortia and intensified bioleaching of chalcopyrite [J]. Biochemical Engineering Journal, 2019, 144: 40−47.

[44] KIM S D, BAE J E, PARK H S, CHA D K. Bioleaching of cadmium and nickel from synthetic sediments by *Acidithiobacillus ferrooxidans* [J]. Environmental Geochemistry and Health, 2005, 27: 229−235.

[45] STEPHAN C, MALTE H, SOREN B, ANTOINE B D, MOHAMED E H, IGOR V P, WOLFGANG S, PAUL W, ANSGAR P, MARIO V, MARK D. Weak iron oxidation by

sulfobacillus thermosulfidooxidans maintains a favorable redox potential for chalcopyrite bioleaching [J]. Frontiers in Microbiology, 2018, 9: 3059.

[46] ZENG Wei-min, QIU Guan-zhou, ZHOU Hong-bo, PENG Juan-hua, CHEN Miao, TAN S N, CHAO Wei-liang, LIU Xue-duan, YANG Yan-sheng. Community structure and dynamics of the free and attached microorganisms during moderately thermophilic bioleaching of chalcopyrite concentrate [J]. Bioresource Technology, 2010, 101: 7068−7075.

[47] CORLISS L M, DONNAY J D H, ELLIOTT N, HASTINGS J M. Symmetry of magnetic structures: Magnetic structure of chalcopyrite [J]. Physical Review, 1958, 112: 1917−1923.

[48] ZHAO Hong-bo, WANG Jun, QIN Wen-qing, ZHENG Xi-hua, TAO Lang, GAN Xiao-wen, QIU Guan-zhou. Surface species of chalcopyrite during bioleaching by moderately thermophilic bacteria [J]. Transactions of Nonferrous Metals Society of China, 2015, 25: 2725−2733.

[49] ZHAO Hong-bo, WANG Jun, GAN Xiao-wen, HU Ming-hao, TAO Lang, QIN Wen-qing, QIU Guan-zhou. Role of pyrite in sulfuric acid leaching of chalcopyrite: An elimination of polysulfide by controlling redox potential [J]. Hydrometallurgy, 2016, 164: 159−165.

[50] ZHAO Hong-bo, WANG Jun, TAO Lang, CAO Pan, YANG Cong-ren, QIN Wen-qing, QIU Guan-zhou. Roles of oxidants and reductants in bioleaching system of chalcopyrite at normal atmospheric pressure and 45 °C [J]. International Journal of Mineral Processing, 2017, 162: 81−91.

[51] WU Shi-fa, YANG Cong-ren, QIN Wen-qing, JIAO Fen, WANG Jun, ZHANG Yan-sheng. Sulfur composition on surface of chalcopyrite during its bioleaching at 50 °C [J]. Transactions of Nonferrous Metals Society of China, 2015, 25: 4110−4118.

[52] ZHAO Hong-bo, HU Ming-hao, LI Yi-ni, ZHU Shan, QIN Wen-qing, QIU Guan-zhou, WANG Jun. Comparison of electrochemical dissolution of chalcopyrite and bornite in acid culture medium [J]. Transactions of Nonferrous Metals Society of China, 2015, 25: 303−313.

[53] YANG Cong-ren, JIAO Fen, QIN Wen-qing. Co-bioleaching of chalcopyrite and silver-bearing bornite in a mixed moderately thermophilic culture [J]. Minerals, 2018, 8: 4.

[54] ZHAO Hong-bo, WANG Jun, YANG Cong-ren, HU Ming-hao, GAN Xiao-wen, TAO Lang, QIN Wen-qing, QIU Guan-zhou. Effect of redox potential on bioleaching of chalcopyrite by moderately thermophilic bacteria: An emphasis on solution compositions [J]. Hydrometallurgy, 2015, 151: 141−150.

[55] GU Guo-hua, HU Ke-ting, ZHANG Xun, XIONG Xian-xue, YANG Hui-sha. The stepwise dissolution of chalcopyrite bioleached by *Leptospirillum ferriphilum* [J]. Electrochimica Acta, 2013, 103: 50−57.

[56] AHMADI A, SCHAFFIE M, MANAFI Z, RANJBAR M. Electrochemical bioleaching of high grade chalcopyrite flotation concentrates in a stirred bioreactor [J]. Hydrometallurgy, 2010, 104: 99−105.

可见光和 Cd^{2+}对黄铜矿生物浸出的催化作用

赵春晓，杨宝军，王星星，赵红波，甘 敏，邱冠周，王 军

中南大学 资源加工与生物工程学院 生物冶金教育部重点实验室，长沙 410083

摘 要：利用扫描电镜(SEM)、同步辐射 X 射线衍射(SR-XRD)和 X 射线光电子能谱(XPS)研究在酸性氧化亚铁硫杆菌存在下，可见光和镉离子(Cd^{2+})对黄铜矿生物浸出的影响。生物浸出 28 天后的结果表明，光照下铜的溶解提高 4.96%；Cd^{2+}单独存在对黄铜矿的浸出有轻微的抑制作用；可见光和 50 mg/L Cd^{2+}同时存在时，溶解铜的浓度提高 14.70%。化学浸出结果表明，可见光能促进体系中铁元素的循环。SEM 结果显示，Cd^{2+}在可见光下促进酸性氧化亚铁杆菌在黄铜矿表面的附着。综合 SR-XRD 和 XPS 结果可知，可见光和 Cd^{2+}促进黄铜矿的浸出，但不会抑制钝化物的形成。提出可见光和 Cd^{2+}对黄铜矿生物浸出协同催化作用机制的模型。

关键词：生物浸出；黄铜矿；Cd^{2+}；酸性氧化亚铁硫杆菌；可见光

(Edited by Bing YANG)